Applied Physics Letters

Electron and hole photoemission detection for band offset determination of tunnel field-effect transistor heterojunctions

Wei Li, Qin Zhang, R. Bijesh, Oleg A. Kirillov, Yiran Liang, Igor Levin, Lian-Mao Peng, Curt A. Richter, Xuelei Liang, S. Datta, David J. Gundlach, and N. V. Nguyen

Citation: Applied Physics Letters **105**, 213501 (2014); doi: 10.1063/1.4902418
View online: http://dx.doi.org/10.1063/1.4902418
View Table of Contents: http://scitation.aip.org/content/aip/journal/apl/105/21?ver=pdfcov
Published by the AIP Publishing

APPLIED PHYSICS LETTERS **105**, 213501 (2014)

Electron and hole photoemission detection for band offset determination of tunnel field-effect transistor heterojunctions

Wei Li,[1,2,a)] Qin Zhang,[1,a)] R. Bijesh,[3] Oleg A. Kirillov,[1] Yiran Liang,[2] Igor Levin,[1] Lian-Mao Peng,[2] Curt A. Richter,[1] Xuelei Liang,[2,b)] S. Datta,[3] David J. Gundlach,[1] and N. V. Nguyen[1,b)]
[1]*National Institute of Standards and Technology, Gaithersburg, Maryland 20899, USA*
[2]*Key Laboratory for the Physics and Chemistry of Nanodevices and Department of Electronics, Peking University, Beijing 100871, China*
[3]*Department of Electrical Engineering, The Pennsylvania State University, University Park, Pennsylvania 16802, USA*

(Received 3 October 2014; accepted 10 November 2014; published online 24 November 2014)

We report experimental methods to ascertain a complete energy band alignment of a broken-gap tunnel field-effect transistor based on an InAs/GaSb hetero-junction. By using graphene as an optically transparent electrode, both the electron and hole barrier heights at the InAs/GaSb interface can be quantified. For a Al_2O_3/InAs/GaSb layer structure, the barrier height from the top of the InAs and GaSb valence bands to the bottom of the Al_2O_3 conduction band is inferred from electron emission whereas hole emissions reveal the barrier height from the top of the Al_2O_3 valence band to the bottom of the InAs and GaSb conduction bands. Subsequently, the offset parameter at the broken gap InAs/GaSb interface is extracted and thus can be used to facilitate the development of predicted models of electron quantum tunneling efficiency and transistor performance. © *2014 AIP Publishing LLC*. [http://dx.doi.org/10.1063/1.4902418]

Different transistor designs for beyond-CMOS technology have been proposed including the tunnel field-effect transistor (TFET),[1] impact-ionization MOS,[2] ferroelectric FET,[3] and electromechanical devices.[4] Prototypes of these devices have been shown to achieve sub-threshold swings less than the 60 mV/decade intrinsic limit of current CMOS at room temperature. Among the candidate designs, the TFET is considered a technologically promising candidate because it offers a much improved on-off current (I_{ON}/I_{OFF}) ratio over a given gate voltage swing and low power consumption.[1] The principle behind such advancement is the adoption of band-to band tunneling (BTBT) as the switching mechanism, instead of thermionic emission which governs conventional CMOS operation in the subthreshold regime. Because BTBT can achieve steeper sub-threshold slopes, lower supply voltages and, thus, less power dissipation can be realized. The most critical challenge in TFET design is to achieve high I_{ON} and low I_{OFF}, while maintaining a subthreshold slope of less than 60 mV/decade. An obvious solution is to use lower band gap and low-effective-mass materials and take advantage of band engineering to increase BTBT. In fact, high I_{ON} at lower voltages was achieved on Ge,[5] InAs, and heterojunction systems such as SiGe/Si,[6] AlGaSb/InAs,[7,8] AlGaAs/InGaAs,[9] and InGaSb/InGaAs.[10] Among these different designs, group III–V heterojunctions are considered to be very promising since they offer small effective masses and their band gaps can be tailored for desired band-edge alignments. Experimental and theoretical studies indicate that the performance of group III-V staggered or broken gap TFETs can be significantly enhanced when compared with homojunctions.[11,12] Because I_{ON} depends on transmission probability over the interband tunneling barrier, which is a function of band offsets, band bending, and other physical parameters at the source and channel interface, it is vital to design a device with appropriate heterojunction band offsets. Thus, having an accurate evaluation or measurement of the band offsets is critical to selecting *a priori* suitable heterojunction materials that will produce the necessary interfacial energy band edge arrangement.

In recent years, IPE has been successful in determining barrier heights at solid/solid interfaces, in particular, semiconductor/insulator and metal/insulator interfaces.[13] IPE on a TFET structure has been shown to be successful in quantifying band alignments of InGaAs/InAs and InAs/p^+AlGaSb.[14,15] In these instances, an IPE experimental procedure was specifically designed and tailored to enhance sensitivity of electron photoemission from each semiconductor component of the heterojunction over a large band gap insulator. In both examples, the measurement technique was possible only when the larger band gap semiconductor is on top of the other. In this letter, we advance the method to a more elaborate approach which simultaneously resolves both valence and conduction band offsets at the heterojunction interface without the restriction of the band gap arrangement used in Zhang's reports.[14,15] Specifically, the offset of the valence bands is determined by electron photoemission, whereas that of conduction bands is measured by hole photoemission. Since hole photoemission is difficult to detect, we use graphene as a unique transparent electrode to enhance the hole emission. This measurement strategy is adopted in this investigation to provide a complete band alignment of a semiconductor heterojunction.

Fig. 1(a) displays a schematic of the TFET InAs/GaSb heterojunction used in the IPE measurement where a bias V_g

a)W. Li and Q. Zhang contributed equally to this work.
b)Author to whom correspondence should be addressed. Electronic addresses: Nhan.Nguyen@nist.gov and liangxl@pku.edu.cn

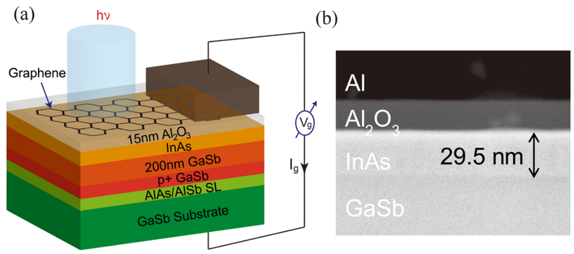

FIG. 1. (a) Schematic of the IPE measurement of the graphene/Al_2O_3/InAs/GaSb structure used in this investigation. The top contact for IPE probe is a thick aluminum. The heterojunction of interest is InAs/GaSb. For more device fabrication details, please see the supplementary material.[35] (b) High-angle annular dark-field STEM image of this heterostructure confirming the layer thickness and interface sharpness.

is applied across the structure and photocurrent (I_g) is measured as a function of photon energy ($h\nu$) of incident light. The IPE quantum yield (Y) is defined as a ratio of photocurrent and incident photon flux. The aim of the measurement is to obtain the barrier height at the buried InAs/GaSb interface. Monolayer graphene is employed as an optically semi-transparent electrode to detect both IPE hole and electron photo-injections. The thickness of InAs was carefully designed to control light absorption and penetration depth in the layer stack and still to maintain the same pseudomorphism at the interface. The high-angle annular dark field image acquired by using scanning transmission electron microscopy (STEM) verifies the layer thickness and interface sharpness (Fig. 1(b)).

Shown in Figs. 2(a) and 2(c) are the cube roots of IPE quantum yield, $Y^{1/3}$, versus photon energy when applied

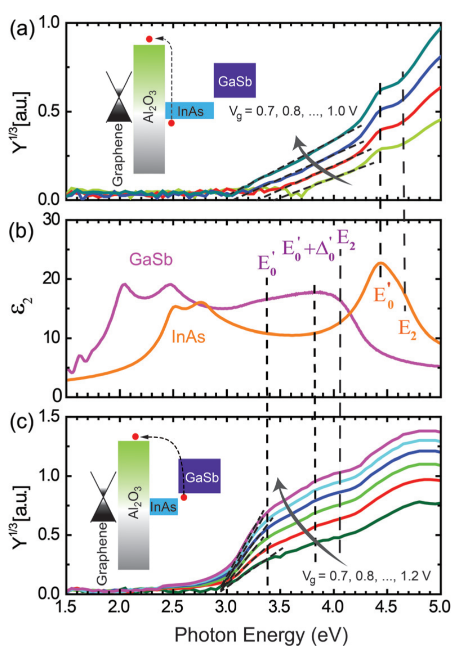

FIG. 2. (a) and (c) are the cube root of the photocurrent yield ($Y^{1/3}$) as a function of photon energy at different gate biases applied between GaSb substrate and aluminum contact for two graphene/Al_2O_3/InAs/GaSb structures, one with 29 nm thick InAs layer and the other 10 nm thick, (b) is the imaginary part $\langle\varepsilon_2\rangle$ of the pseudo-dielectric function of InAs (orange) and GaSb (magenta) measured by spectroscopic ellipsometry.

$V_g > V_{FB}$, where V_{FB} is the flatband voltage, for the heterojunction with a 29 nm and 10 nm InAs layer, respectively. The flatband voltage is equivalent to an externally applied potential at which the photocurrent switches the polarity or when the internal electric field in the oxide layer becomes zero. The electric field across the oxide is estimated by (V_g-V_{FB})/(Al_2O_3 thickness) assuming the voltage drops entirely inside the oxide.[14] Following the classical Powell model,[16] $Y^{1/3}$ is a linear function of photon energy above and near the spectral threshold for semiconductor/insulator interface. The electrons escaping over the oxide conduction band under light illumination are photo-excited in the InAs and/or GaSb layer. Discerning the source of material where these electrons emerge from can be carried out by observing whether the photoemission quantum yield contains optical absorption features belonging specifically to that material. For semiconductors, the most common and unique features in the visible and ultraviolet part of optical absorption spectrum are associated with the inter-band transition critical points (CPs).[17] The CPs of InAs and GaSb are recognized from their dielectric functions shown in Fig. 2(b), which are measured by spectroscopic ellipsometry.[13,18,19] CPs relevant to IPE data interpretation are those of E_0', $E_0' + \Delta_0'$, and E_2 transitions indicated in Fig. 2(b) of the imaginary part (ε_2) of the dielectric functions. The IPE yield from 29 nm InAs sample contains E_0' (~4.4 eV) and E_2 (~4.6 eV) being direct transitions from the valence band to the conduction band at the Γ and X point of the Brillouin zone, respectively.[20] With a high optical absorption in the range of E_0' and E_2 point, it is expected that the quantum yield will be enhanced. However, in the vicinity of E_0', the yield increases faster with the increase in photon energy and deviates from the preceding linear region; displaying a bump. At both of these two CPs, the quantum efficiency shows a different trend, whereas at E_2, the yield remains unchanged. These different trends can be explained by how the band structure at E_0' and E_2 of InAs lines up with the large band gap of Al_2O_3. Fig. S1 (supplementary material) displays a schematic of the band structure of InAs that is so arranged in relation with the valence and conduction band of Al_2O_3. E_0' associates with the direct interband transition from the top of valence band at Γ point to the bottom of higher conduction band (indicated by vertical line E_0' in Fig. S1), indicating the photo-excited electrons in final state of higher energy above the conduction band edge of Al_2O_3, thereby, contributing to and enhancing the photo-electron yield. On the contrary, the final state (indicated by vertical line E_2 in Fig. S1) of photo-excited electrons at the X point lies below the conduction band edge of Al_2O_3 thus contributing no photoelectrons to the IPE yield. Furthermore, none of GaSb CPs appears in the photoemission spectrum since, for photon energies near the barrier height threshold, the incidence light is mostly absorbed in the 29 nm InAs layer and less than 5% of incident light can penetrate into GaSb for photon energy larger than 2.7 eV.[15] Therefore, it can be safely concluded that the photocurrents originate mainly from the InAs layer. In contrast, Fig. 2(c) presents the IPE $Y^{1/3}$ for a much thinner (10 nm) InAs layer sample which allows most light transmitted into the GaSb layer. It contains three CPs (E_0', $E_0' + \Delta_0'$, and E_2) corresponding to GaSb absorption features, where E_0' and $E_0' + \Delta_0'$

correspond to direct gap transitions and the spin-orbit splitting at the Γ point in the Brillouin zone, respectively, and the E_2 feature is due to transitions along Σ or near the X point.[21,22] Thus, we deduce that the photocurrents are due to photoemission from the GaSb. From these observations, it is concluded that the lower thresholds in Fig. 2(a) are the barrier heights from the InAs valence band maximum to the Al_2O_3 conduction band minimum and the higher thresholds in Fig. 2(c) are the barrier heights from the GaSb valence band maximum to the Al_2O_3 conduction band minimum.

The barrier heights for electron photoemissions ($V_g > V_{FB}$), extracted from Figs. 2(a) and 2(c), are observed to be field dependent due to the image force lowering effect.[23] The lowering appears to be a greater effect for the InAs layer adjacent to the oxide and lesser for the farther GaSb layer. The flatband or *zero*-field barrier height (Φ_0) can be determined by the linear relationship of Schottky plot of barrier height vs. square-root of electric field as shown in Fig. 3. As a result, Φ_0 from the InAs and GaSb valence band maximum to the Al_2O_3 conduction band minimum is determined to be 3.45 eV and 2.92 eV with a 0.05 eV uncertainty. The band offset at InAs and GaSb interface can be deduced from their conduction band offsets with respect to the valence band of Al_2O_3. They can be conclusively determined by measuring the corresponding hole barrier heights.

In a traditional IPE measurement, the hole photocurrent (if present) from semiconductor is negligible due to its much lower quantum yield compared to the electron photocurrent from the semi-transparent gate (usually thin metal).[24] However, Yan *et al.*[25] first reported that by using graphene as a transparent electrode, one can greatly enhance the detection sensitivity to hole photoemission. The main advantages of using graphene as a transparent electrode to facilitate hole photocurrent measurements are described in the following. In conventional IPE measurements, the electron photoemission from a thin layer of metal which is used as a semi-transparent electrode normally overwhelms the hole emission from the semiconductor substrate. Replacing the metal with a graphene monolayer which has a broad range light

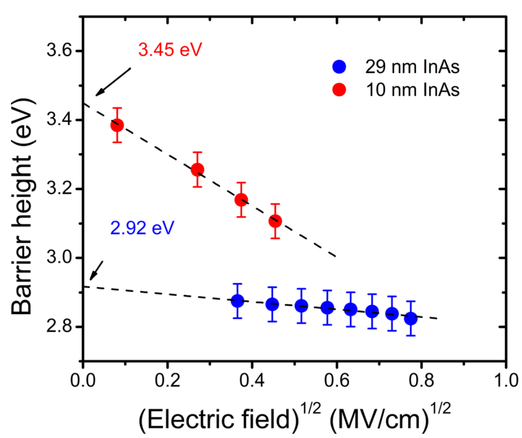

FIG. 3. Schottky plot of the barrier height as a function of square root of oxide electric field. Dash line is a linear fit to determine the zero-field barrier height (Φ_0) at the oxide flat band condition. $\Phi_0 = 3.45\,\text{eV} \pm 0.05\,\text{eV}$ and $2.92\,\text{eV} \pm 0.05\,\text{eV}$ is the barrier height from the InAs and GaSb valence band maximum to the Al_2O_3.

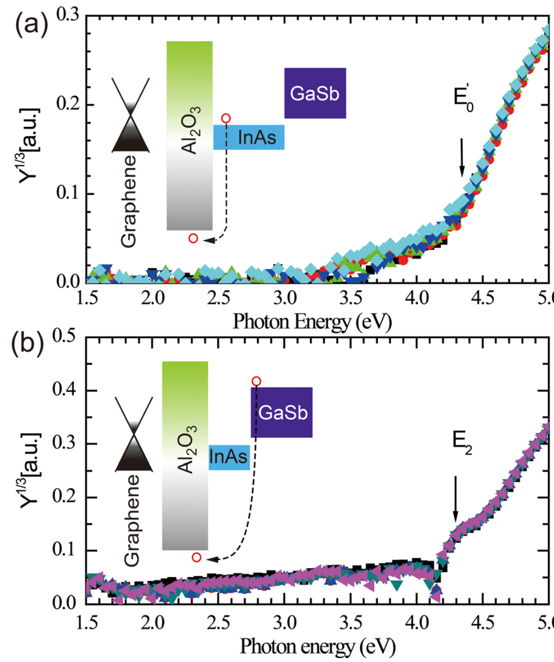

FIG. 4. The cube root of the photocurrent yield due to hole emission from (a) InAs and (b) GaSb as a function of photon energy at different gate biases.

transmittance as high as 97.7% [26] allows most of the incident photon flux to reach the emitter thus minimizing electron injection from the graphene electrode,[27] and increases the external quantum efficiency of the hole emission. In addition, the resistivity of pristine graphene has been estimated to be as low as $10^{-6}\,\Omega\,\text{cm}$, which is lower than a silver electrode, and the sheet resistance of monolayer graphene can be $30\Omega/\square$ at room temperature, which is comparable to a highly conducting transparent electrode such as indium tin oxide.[28] The high electrical conductivity of graphene makes the collection of the emitted carriers more efficient and decreases carrier recombination. As a result, shown in Fig. 4(a) are photon current yields of the hole emissions for the thick InAs layer sample. Since this layer absorbs most of the incident light, the observed photo-excited hole emission comes from the InAs layer; thus, the threshold corresponds to the barrier height from the InAs conduction band to the Al_2O_3 valence band. Unlike electron photoemission

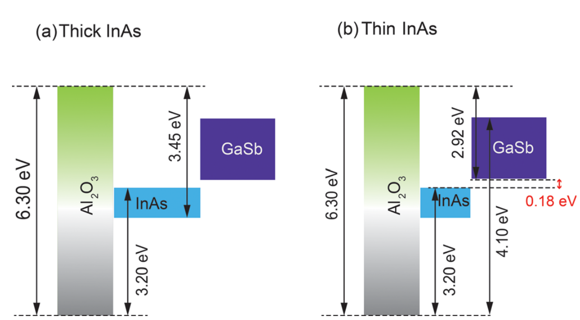

FIG. 5. The band alignment (not to scale) of broken-gap InAs and GaSb heterojunction at the oxide zero field: (a) thick InAs and (b) thin InAs.

TABLE I. Comparison of the extracted conduction (ΔE_c) and valence (ΔE_v) band offset at the Al_2O_3/InAs, Al_2O_3/GaSb, and InAs/GaSb interface with the reported values.

	Al_2O_3/InAs		Al_2O_3/GaSb		InAs/GaSb	
	This work	Others	This work	Others	This work	Others
ΔE_c (eV)	3.09	2.88 (Ref. 15)	2.24	2.3 (Ref. 32)	0.86	0.93 (Refs. 33 and 34)
ΔE_v (eV)	2.84	…	3.42	3.05 (Ref. 32)	0.54	0.51 (Refs. 33 and 34)

thresholds, hole photoemission thresholds appear to be field-independent. Further theoretical investigation should be taken to explain this observation. A similar independence on electric field has been observed in other material systems.[29,30] Consequently, from Fig. 4(a), the field-independent band offset from InAs conduction band minimum to the Al_2O_3 valence band maximum is found to be 3.20 eV. In the case of the thin InAs layer sample, mainly hole emission from GaSb layer is observed, and the barrier height from the GaSb conduction band minimum to the Al_2O_3 valence band maximum is 4.10 eV as shown in Fig. 4(b). The IPE yield spectrum from the thick InAs layer sample features a signature of InAs as shown by the absorption peak E_0' in Fig. 2(b). At the photon energy of this critical point, the hole emission is enhanced and can be associated with the direct E_0' optical excitation of InAs. On the other hand, the plateau seen in the quantum yield of the thin InAs sample near 4.3 eV (see Fig. 4(b))—corresponding to the E_2 feature, a transition along Σ or near the X point of GaSb—may indicate a lesser contribution of the excited holes to photo emission yield because their final state may lie below the valence band edge of Al_2O_3.

From the *zero*-field barriers determined in the above band diagram of thick and thin InAs layer, the InAs/GaSb broken-gap hetero-junction can be schematically established as shown in Figs. 5(a) and 5(b). Table I summarizes and compares the conduction band ($\mathbf{\Delta E_c}$) and valence band ($\mathbf{\Delta E_v}$) offsets determined from the corresponding measured barrier heights and band gaps (see Fig. 5) from this study with previously reported values, where we define $\mathbf{\Delta E_c}$ and $\mathbf{\Delta E_v}$ as the band discontinuity of conduction bands and valence bands, respectively. As mentioned before, only the results in this work provide both the electron and hole barrier heights. It is interesting to verify the consistency of the IPE barrier height results by comparing the band gap of Al_2O_3 of 6.29 eV calculated from the band alignment with the band gap of 6.30 eV independently determined from an optical absorption measurement on the same Al_2O_3.[31] Finally, the broken gap of ~ -0.18 eV between the conduction band edge of InAs and the valence band edge of GaSb is extracted from the band diagram in Fig. 5.

In summary, we demonstrate the strength of IPE measurements to quantitatively characterize both the electron and hole barrier heights in the heterojunction of a TFET. Taking advantage of the high transmissivity and conductivity of monolayer graphene and using it as a transparent electrode for IPE measurements, we are able to detect holes photo-injected over an interface barrier. By sequentially measuring the electron and hole photoemission currents, we are able to determine the energetic barrier heights at the heterojunction interface, and derive the complete and quantitative electronic band alignment. The knowledge infrastructure established here provides critical physical input parameters to facilitate the design and advancement of heterojunction TFETs. The methodology reported here to construct the band alignment of InAs and GaSb broken-gap heterojunction are broadly applicable to other heterojuction materials systems and device technologies, e.g., solar cells.

This work was supported by the Ministry of Science and Technology of China (Grant No. 2011CB921904) and the Ministry of education of China (Grant No. 113003A). W.L. was partly supported by the National Institute of Standards and Technology. The authors would like to acknowledge NIST NanoFab's support for device fabrications.

[1]A. C. Seabaugh and Q. Zhang, Proc. IEEE **98**, 2095 (2010).
[2]K. Gopalakrishnan, P. B. Griffin, and J. D. Plummer, in *IEDM'02 International Electron Devices Meeting* (IEEE, 2002), pp. 289–292.
[3]S. Salahuddin and S. Datta, Nano Lett. **8**, 405 (2008).
[4]H. Kam, D. T. Lee, R. T. Howe, and T.-J. King, in *IEEE International Electron Devices Meeting (IEDM)* (IEEE, 2005), pp. 463–466.
[5]A. Bowonder, P. Patel, K. Jeon, J. Oh, P. Majhi, H.-H. Tseng, and C. Hu, in *8th International Workshop on Junction Technology* (IEEE, 2009), p. 93.
[6]O. M. Nayfeh, C. N. Chleirigh, J. Hennessy, L. Gomez, J. L. Hoyt, and D. A. Antoniadis, IEEE Electron Device Lett. **29**, 1074 (2008).
[7]S. O. Koswatta, S. J. Koester, and W. Haensch, in *IEEE International Electron Devices Meeting (IEDM)* (IEEE, 2009), pp. 909–912.
[8]J. Knoch and J. Appenzeller, Electron Device Lett. **31**, 305 (2010).
[9]L. Q. Wang, E. Yu, Y. Taur, and P. Asbeck, IEEE Electron Device Lett. **31**, 431 (2010).
[10]D. K. Mohata, R. Bijesh, Y. Zhu, M. K. Hudait, R. Southwick, Z. Chbili, D. Gundlach, J. Suehle, J. M. Fastenau, D. Loubychev, A. K. Liu, T. S. Mayer, V. Narayanan, and S. Datta, in *2012 Symposium on VLSI Technology (VLSIT)* (IEEE, 2012), pp. 53–54.
[11]J. Knoch, S. Mantl, and J. Appenzeller, Solid State Electron. **51**, 572 (2007).
[12]B. Rajamohanan, D. Mohata, Y. Zhu, M. Hudait, Z. Jiang, M. Hollander, G. Klimeck, and S. Datta, J. Appl. Phys. **115**, 044502 (2014).
[13]V. V. Afanas'ev, *Internal Photoemission Spectroscopy: Principles and Applications* (Elsevier, Amsterdam, 2008).
[14]Q. Zhang, G. Zhou, H. G. Xing, A. C. Seabaugh, K. Xu, H. Sio, O. A. Kirillov, C. A. Richter, and N. V. Nguyen, Appl. Phys. Lett. **100**, 102104 (2012).
[15]Q. Zhang, R. Li, R. Yan, T. Kosel, H. G. Xing, A. C. Seabaugh, K. Xu, O. A. Kirillov, D. J. Gundlach, C. A. Richter, and N. V. Nguyen, Appl. Phys. Lett. **102**, 012101 (2013).
[16]R. J. Powell, J. Appl. Phys. **41**, 2424 (1970).
[17]P. Y. Yu and M. Cardona, *Fundamentals of Semiconductors*, 2nd ed. (Springer-Verlag, New York, 1999).
[18]V. V. Afanas'ev and A. Stesmans, J. Appl. Phys. **102**, 081301 (2007).
[19]N. V. Nguyen, M. Xu, O. A. Kirillov, P. D. Ye, C. Wang, K. Cheung, and J. S. Suehle, Appl. Phys. Lett. **96**, 052107 (2010).
[20]T. J. Kim, J. J. Yoon, S. Y. Hwang, Y. W. Jung, T. H. Ghong, Y. D. Kim, H. Kim, and Y.-C. Chang, Appl. Phys. Lett. **97**, 171912 (2010).
[21]T. Chiang and D. Eastman, Phys. Rev. B **22**, 2940 (1980).
[22]M. Munoz, K. Wei, and H. Pollak, Phys. Rev. B **60**, 8105 (1999).
[23]S. M. Sze and K. K. NG, in *Physics of Semiconductor Devices* (John Wiley and Sons, Inc., New Jersey, 2007).
[24]R. J. Powell, J. Appl. Phys. **40**, 5093 (1969).

[25]R. Yan, Q. Zhang, O. A. Kirillov, W. Li, J. Basham, A. Boosalis, X. Liang, D. Jena, C. A. Richter, A. Seabaugh, D. J. Gundlach, H. G. Xing, and N. V. Nguyen, Appl. Phys. Lett. **102**, 123106 (2013).
[26]R. R. Nair, P. Blake, A. N. Grigorenko, K. S. Novoselov, T. J. Booth, T. Stauber, N. M. R. Peres, and A. K. Geim, Science **320**, 1308 (2008).
[27]K. Xu, C. F. Zeng, Q. Zhang, R. S. Yan, P. D. Ye, K. Wang, A. C. Seabaugh, H. G. Xing, J. S. Suehle, C. A. Richter, D. J. Gundlach, and N. V. Nguyen, Nano Lett. **13**, 131 (2013).
[28]J. H. Chen, C. Jang, S. Xiao, M. Ishigami, and M. S. Fuhrer, Nat. Nanotechnol. **3**, 206 (2008).
[29]R. Yan, Q. Zhang, W. Li, I. Calizo, T. Shen, C. A. Richter, A. R. Hight-Walker, X. Liang, A. Seabaugh, D. Jena, H. Grace Xing, D. J. Gundlach, and N. V. Nguyen, Appl. Phys. Lett. **101**, 022105 (2012).
[30]R. Bijesh, H. Liu, H. Madan, D. Mohata, W. Li, N. V. Nguyen, D. Gundlach, C. A. Richter, J. Maier, K. Wang, T. Clarke, J. M. Fastenau, D. Loubychev, W. K. Liu, V. Narayanan, and S. Datta, in *IEEE International Electron Devices Meeting (IEDM)* (IEEE, 2013), pp. 28.22.21–28.22.24.
[31]N. V. Nguyen, S. Sayan, I. Levin, J. R. Ehrstein, I. J. R. Baumvol, C. Driemeier, C. Krug, L. Wielunski, P. Y. Hung, and A. Diebold, J. Vac. Sci. Technol. A **23**, 1706 (2005).
[32]V. V. Afanas'ev, H. Y. Chou, A. Stesmans, C. Merckling, and X. Sun, Appl. Phys. Lett. **98**, 072102 (2011).
[33]H. Kroemer, Physica E **20**, 196 (2004).
[34]I. Vurgaftman, J. R. Meyer, and L.-R. Ram-Mohan, J. Appl. Phys. **89**, 5815 (2001).
[35]See supplementary material at http://dx.doi.org/10.1063/1.4902418 for device fabrication and measurement details.